Parasequence geometry and facies architecture in the upper Cretaceous Point Lookout Sandstone, Four Corners platform, southwestern Colorado

Danny R. Katzman and Robyn. Wright-Dunbar

1992, pp. 187-197. https://doi.org/10.56577/FFC-43.187

in:

San Juan Basin IV, Lucas, S. G.; Kues, B. S.; Williamson, T. E.; Hunt, A. P.; [eds.], New Mexico Geological Society 43rd Annual Fall Field Conference Guidebook, 411 p. https://doi.org/10.56577/FFC-43

This page is intentionally left blank to maintain order of facing pages.

PARASEQUENCE GEOMETRY AND FACIES ARCHITECTURE IN THE UPPER CRETACEOUS POINT LOOKOUT SANDSTONE, FOUR CORNERS PLATFORM, SOUTHWESTERN COLORADO

DANNY KATZMAN[1] and ROBYN WRIGHT-DUNBAR[2]
[1]New Mexico Environment Department, 525 Camino de los Marquez, Santa Fe, New Mexico 87502-6610;
[2]Department of Geology and Geophysics, Rice University, Houston, Texas 77251-1892

Abstract—In the Upper Cretaceous Point Lookout Sandstone in southwestern Colorado, the presence of distinctly different scales of transgressive deposits defines a hierarchy of high-frequency, nearshore-marine transgressive-regressive cycles. The two cycle scales, parasequences and parasequence sets, are delineated on the basis of thickness and lithologic characteristics of the transgressive deposits at inner-shelf and back-barrier positions. This observation is contrary to most previous work on cycles at this scale, which suggests that the stratigraphic record is composed of regressive strata with the transgressive portion of the cycle being represented only by a surface of erosion or nondeposition. Here, we recognize that both regressive and transgressive deposits are important components of the cycle stratigraphy.

INTRODUCTION

Parasequences are relatively conformable successions of strata deposited in response to high-frequency (10^4–10^6 years) oscillations in relative sea level (van Wagoner et al., 1988). They are the high-frequency, transgressive-regressive (T-R) depositional cycles that comprise the fundamental building blocks of large-scale, nearshore-marine sandstones (Hollenshead and Pritchard, 1961; Ryer, 1977).

Deposits of the Upper Cretaceous Point Lookout Sandstone in the northwestern San Juan Basin record high-frequency T-R cycles within an overall regressive sheet sandstone. Two scales of T-R cycles are recognized on the basis of sandstone geometry and transgressive deposits. Two stacked progradational parasequence sets are each internally composed of four progradational parasequences, the latter of which likely represents durations of between <50 ky to 100 ky. This range is based on an estimate of the total number of parasequences comprising the Point Lookout regression, divided into the total duration of regression (using ammonite zones, Fouch et al., 1983), to derive an average minimum and maximum duration of individual parasequences (Wright, 1984, 1986).

Most previous work on parasequence models (e.g., Hollenshead and Pritchard, 1961; van Wagoner, 1985; van Wagoner et al., 1988; Ryer, 1977) suggests that the entire parasequence record consists of regressive strata, with little or no record of the transgressive phase. In contrast, modifications on the "classic" parasequence model have been proposed recently for the Point Lookout Sandstone that characterize the transgressive phase of parasequences as depositional (Devine, 1980, 1991; Wright, 1988; Wright and Hayden, 1988). The Point Lookout in the study area contains transgressive deposits, at both inner-shelf and back-barrier positions, that comprise a volumetrically significant portion of the cycle stratigraphy. Thus, distinguishing transgressive deposits from regressive deposits becomes important in the understanding of cycle geometry, facies architecture and in paleoenvironmental reconstructions. This paper demonstrates the nature of the hierarchical arrangement of Point Lookout Sandstone parasequences, documents the products of transgression and regression at parasequence and parasequence-set scales, and develops criteria for differentiating transgressive and regressive deposits. Results are based on outcrop exposures of one parasequence-set boundary and the underlying and overlying parasequence sets.

Detailed study of the three-dimensional geometry of parasequences and their internal components provides important information that may ultimately lead to a better understanding of the relative roles of glacio-eustacy (de Boer and Wonders, 1984), autogenic deltaic processes (Swift et al., 1984), tectonics, and climate (van Wagoner et al., 1990) that interact to produce parasequences and associated stacking patterns. In addition, delineation of parasequence geometry has direct implications for the study of vertical porosity and permeability heterogeneities in reservoir sandstones, because thin mudstones that often occur on transgressive surfaces at parasequence or parasequence-set boundaries can effectively compartmentalize an otherwise relatively homogeneous reservoir sandstone.

SETTING AND METHODOLOGY

The Point Lookout Sandstone is the regressive portion of a large-scale regressive-transgressive cycle (the Mesaverde Group) deposited in late Santonian–early Campanian time along the western margin of the Western Interior Basin of the United States. The Point Lookout Sandstone interfingers with both the underlying marine Mancos Shale and the overlying, predominantly nonmarine, Menefee Formation (Fig. 1). This study focuses on exposures that form prominent mesas just east of U.S. Highway 666 between Towaoc, Colorado, and the New Mexico state line (Fig. 2).

Regional paleoshoreline trend in the Point Lookout Sandstone was approximately NW-SE (Sears et al., 1941), and has been constrained on a local basis with aero-rad surveys (Zech, personal comm. 1989) The depositional basin was to the northeast. Excellent three-dimensional exposures in Mancos Canyon, Tanner Canyon and Head Draw permit correlation of key surfaces and facies along depositional strike and dip. Initial correlation of prominent stratigraphic breaks (i.e., transgressive surfaces) was done predominantly with low-altitude oblique aerial photographs and outcrop photographs. In most cases, especially in Mancos Canyon, it was possible to physically trace correlation surfaces.

Thirteen sections were measured and described in the study area and field observations were made at numerous additional localities (Fig. 2). Bed thickness and geometry, paleocurrent information, internal stratification type, and bioturbation type were all recorded in the field. Grain size and sorting were also determined using a field grain-size card. Facies interpretations were based largely on field data, but were also distinguished petrographically by qualitatively examining sandstone mineralogy, sorting and types of post-depositional cement.

SANDSTONE LITHOFACIES

The Point Lookout Sandstone in the study area is divided into four primary lithofacies and several subfacies on the basis of textural trends, lithology, ichnofacies and sedimentary structures. The characteristics of each lithofacies and environmental interpretations are shown in Table 1.

Lithofacies Ia–c

Description

Lithofacies Ia (LF Ia) is the most common and widespread facies of the Point Lookout Sandstone in the study area. LF Ia occurs as laterally continuous sandstone bodies that commonly display a coarsening-upward textural trend and achieve a maximum thickness of 7 m. Sandstone of LF Ia is bounded above and below by transgressive surfaces (= marine-flooding surfaces), with or without lithofacies III (LF III)

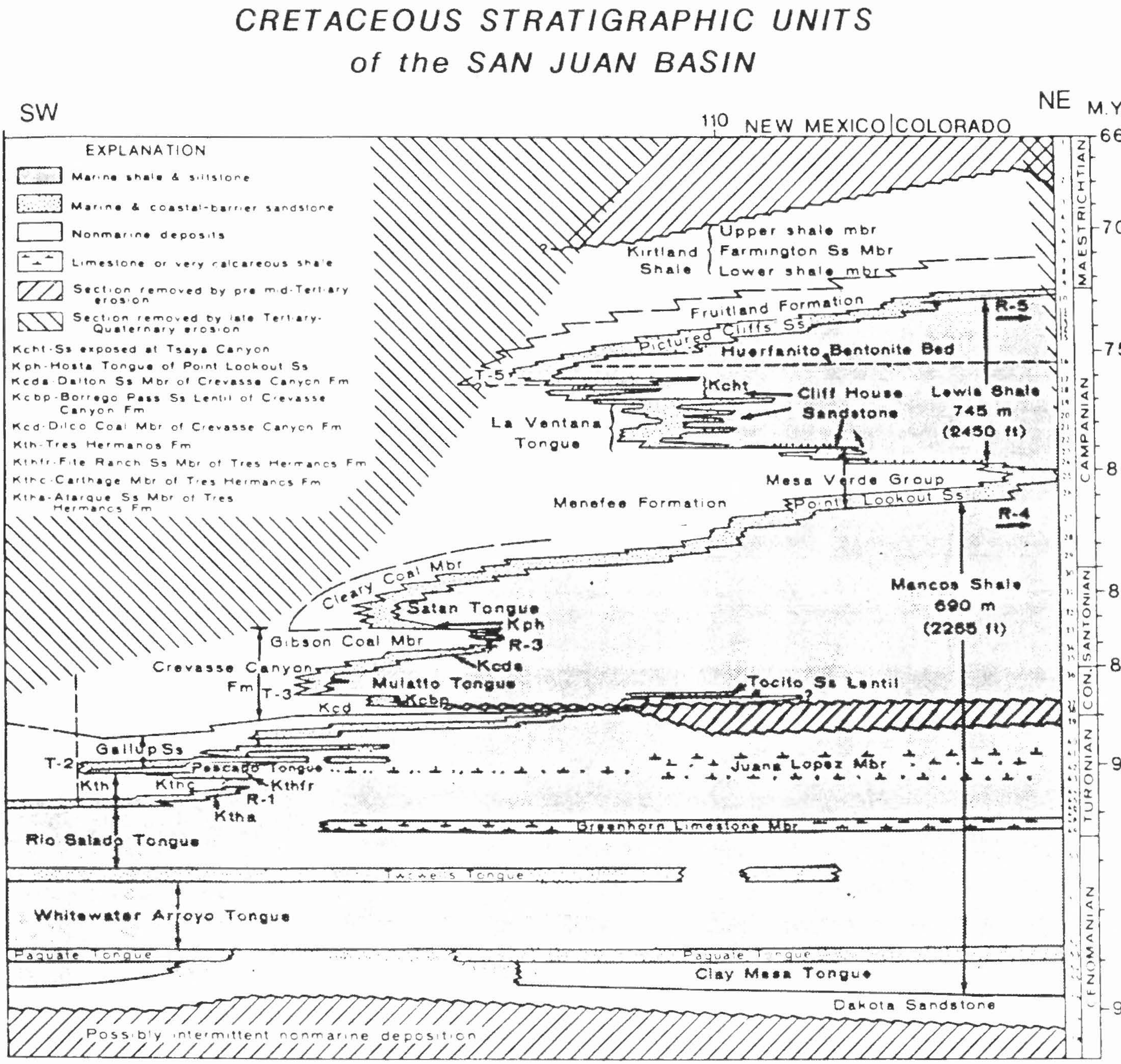

FIGURE 1. Regional stratigraphic section of Upper Cretaceous strata of the San Juan Basin (from Molenaar, 1983).

mudstone. Stratification in LF Ia consists predominantly of basal hummocky cross-stratified sandstone grading upward into swaley cross-stratification and subordinant low-angle parallel laminations. Symmetrical ripple marks cap some beds, mainly within the hummocky cross-stratified portion. LF Ia occurs as individual coarsening-upward sheet sandstones, or as stacked sets of up to four coarsening-upward amalgamated sheet sandstones bounded by marine-flooding surfaces and inner-shelf sandstones of LF IV. Bioturbation is common in the basal portion of LF Ia and decreases upward. Characteristic trace fossils are *Ophiomorpha, Thalassinoides* and *Planolites*.

Associated with LF Ia are subfacies LF Ib and LF Ic, which occur on a limited basis within the study area. LF Ib consists of fine- to medium-grained sandstone with low-angle parallel laminations that dip less than 5° in the seaward direction. Where preserved, sandstones of LF Ib gradationally overlie LF Ia and attain a maximum thickness of 2 m. Locally, heavy minerals are concentrated along laminations. *Ophiomorpha* burrows occur sparsely within LF Ib.

LF Ic consists of thinly interbedded siltstone and very fine-grained sandstone and is transitional updip with sandstones of LF Ia. Sandstones within LF Ic are generally less than 1 m thick (more commonly less than 30 cm thick) and interfinger with siltstones in the seaward direction. These sandstones are sharp based, contain predominantly parallel laminations and hummocky cross-stratification, and commonly have symmetrical ripple marks on the upper surface. Tool marks on the base of sandstones indicate offshore and alongshore current directions. The trace fossil *Planolites* is common within LF Ic.

Interpretation

LF Ia–c represent deposition by a prograding barrier or strandline (Reinson, 1984). Progressing in a seaward direction, LF Ib represents

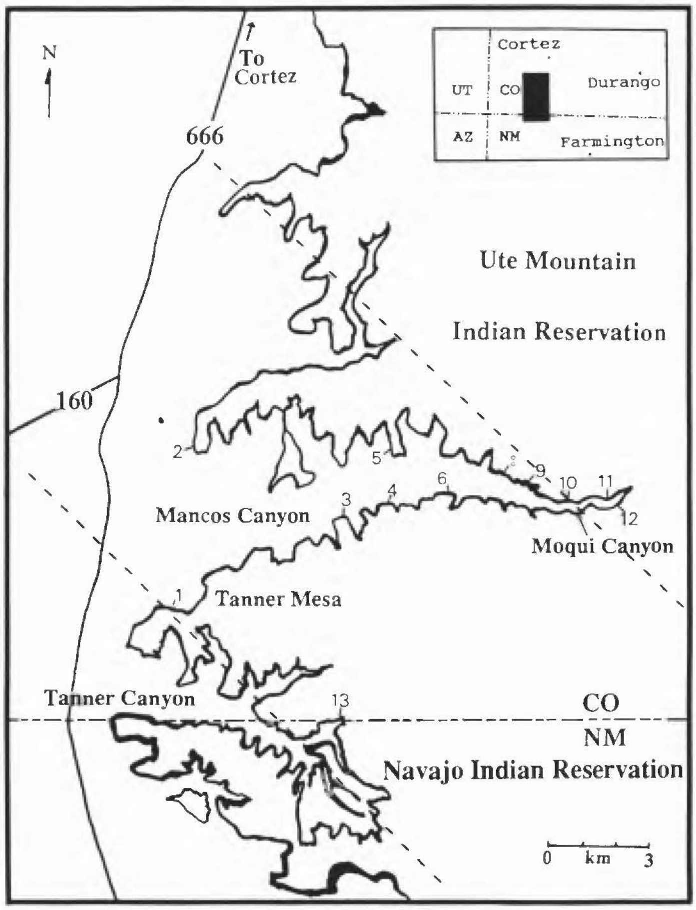

FIGURE 2. Location map of Point Lookout outcrop belt in the study area. Numbers refer to measured section localities. Dashed lines correspond to major shoreline trends at parasequence-set boundaries at Tanner Mesa and Moqui Canyon.

FIGURE 3. Shoreface sandstone (LF Ia) erosionally overlain by fluvial and tidal channels of LF IIa. Arrows point to the contact at the base of a channel-fill sandstone.

foreshore or swash platform, LF Ia represents upper and lower shoreface, and LF Ic represents the offshore transition to the inner shelf. The predominance of hummocky and swaley cross-stratification (LF Ia) and the absence of trough and tabular cross-stratification in the shoreface zone suggests that most of the shoreface was susceptible to combined flow conditions (Harms et al., 1975, 1982), and that storm processes dominated over wave-driven currents in the entire shoreface (Montz et al., 1985; Leckie and Walker, 1982; Oomkens, 1974).

Lithofacies IIa–c

Description

LF IIa–c forms widespread sandstone sheets (up to 15 m thick) comprising a variety of sandstone body geometries. LF IIa is up to 7 m thick and is characterized by poorly sorted stacked channel sandstones (<2 m thick) and minor carbonaceous mudstones. Sandstones of LF IIa erosionally overlie LF Ia shoreface sandstone (Fig. 3). The channel sandstones contain predominantly offshore- and alongshore-oriented trough and tabular cross-stratification, and parallel laminations. Mud rip-ups are common throughout LF IIa, and mud drapes (largely organic debris) occur on toe sets of some crossbeds (Fig. 4A). Some channels have large-scale lateral accretion surfaces (Fig. 4B). LF IIa contains locally abundant marine trace fossils *Arenicolites* and *Planolites* and sparse amounts of the brackish-water trace fossils of the pelecypod *Teredo*.

LF IIb consists of thinly laminated, very fine- to fine-grained sandstone and carbonaceous siltstone (Fig. 5A and 5B), and achieves a maximum thickness of 1 m. LF IIb lies in sharp contact on LF IIa and is present only at the seaward extent of LF IIa. Sandstone beds are generally less than 20 cm thick and laterally discontinuous over several meters. These sharp-based sandstones are parallel laminated and commonly contain mud rip-ups. Symmetrical ripple marks and root traces frequently occur on the top of sandstones. Some sandstones at the top of LF IIb show load deformation. Finer-grained portions of LF IIb contain organic material, from fine flakes to pieces of wood up to 1 meter in length, and a few beds up to 10 cm thick, of nearly pure organic matter (peat?) containing abundant mica flakes. Trace fossils

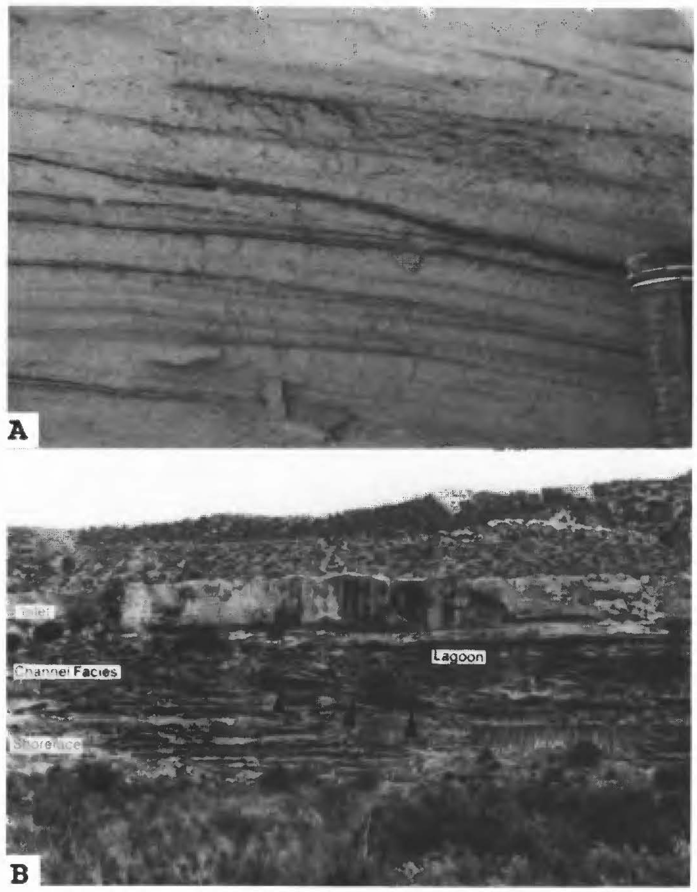

FIGURE 4. Depositional structures in LF Ia. A, Double mud drapes. The drapes in this example are composed of very fine organic detritus. B, Large-scale lateral accretion surfaces that lie in erosional contact with shoreface sandstone (LF Ia). Arrows delineate a single lateral accretion surface.

TABLE 1. Compilation of Point Lookout Sandstone sedimentary facies, structures, ichnofacies and depositional environments.

LITHOFACIES CODE	LITHOLOGY	SANDSTONE STRATIFICATION TYPES	ICHNOFAUNA	INTERPRETATION
LF Ia	Very fine- to fine-grained sandstone	HCS and SCS, minor low-angle, parallel lams.	*Ophiomorpha* *Planolites* *Thalassinoides*	Shoreface
LF Ib	medium-grained sandstone	parallel lams.	*Ophiomorpha*	foreshore
LF Ic	thinly inter-bedded fine-grained sand-stone and siltstone	HCS and parallel lams.	*Planolites*	offshore transi-tion to inner shelf
LF IIa	Fine- to very coarse-grained sandstone, minor silt-stone	trough and tabular cross-strat; parallel lams.	*Skolithos* *Arenicolites* *Planolites* *Macaronichnus*	fluvial channels and tidal creeks
LF IIb	Very fine- to fine-grained sandstone and siltstone	parallel lams. ripple marks	*Planolites* *Teredo*	lagoon
LF IIc	medium-grained sandstone	trough and tabular cross-strat, parallel lams.		tidal inlet and tidal delta
LF III	Thinly inter-bedded very fine-grained sandstone and siltstone	HCS and SCS, wave-rippled tops	*Chondrites* *Planolites* *Thalassinoides*	Parasequence-scale trans-gressive deposits
LF IV	Coalesced very fine- to fine-grained sandstone	HCS and SCS, parallel lams, wave-rippled tops	*Planolites* *Thalassinoides*	Parasequence-set scale, transgressive inner-shelf shoal complex

characteristic of LF IIb are *Planolites* and burrows of *Teredo*. No body fossils have been found.

LF IIc consists of well-sorted, cross-stratified sandstone, lies in sharp (erosional) contact on LF IIb mudstones and sandstones, and achieves a maximum thickness of 7 m. LF IIc consists of broad channel forms up to 0.5 km wide and laterally equivalent smaller (<50 m wide) stacked channel forms. Crossbedding within the large channel forms of LF IIc consists of predominantly bidirectional (herringbone?) trough and planar cross-stratification (up to 1 m in height) at the base, grading upward into smaller-scale bidirectional (herringbone?) cross-stratification and minor parallel laminations (Fig. 6A). This cross-stratification is superimposed on dipping (approximately 17°) lateral accretion surfaces. Reactivation surfaces and mud drapes are common. The large channel forms interfinger laterally (landward) with smaller, stacked channel forms with predominantly offshore- or onshore-oriented trough and planar cross-stratification (Fig. 6B). These channels also interfinger landward with sandstones and mudstones of LF IIb (Fig. 6C). Root traces in sandstone are common near the top of LF IIc. Textural characteristics of LF IIc sandstone are similar to those of foreshore (LF Ic) and upper shoreface (upper LF Ia) deposits, suggesting sediment exchange between the two environments.

Interpretation

LF IIa–c are interpreted to represent a variety of back-barrier and backshore subenvironments. Channel sandstones of LF IIa represent the lateral migration and aggradation of coastal-plain channels. The channels locally show tidal influence in the form of mud drapes and bidirectional crossbedding. Variable marine (estuarine) influence is indicated by marine and brackish trace fossils, suggesting that some of these channels were open to tidal exchange while others were fluvial dominated. These channels lie erosionally on top of upper shoreface deposits (LF Ia), in the position that foreshore deposits (LF Ib) might otherwise occupy. This suggests that these channels were responsible for removal of the foreshore deposits (except at positions that shorelines occupied during maximum transgression) by lateral migration during progradation. They are, therefore, interpreted to represent the source of sediment for shoreface progradation. The maximum thickness of LF IIa (up to 7 m, locally) is greater than that of individual channels (<2 m thick), suggesting that channel aggradation occurred in response to relative baselevel rise.

The limited areal extent of LF IIb suggests that the facies represents small lagoon or pond deposits, or that significant erosion of these deposits occurred during transgressive ravinement. The occurrence of *Teredo* burrows suggests brackish-water conditions. Thin, sharp-based sandstones with wave-rippled tops, mud rip-ups, and load-deformed sandstones suggest that storm processes and washover deposition were important processes.

LF IIc is interpreted to represent tidal channel, tidal inlet, and flood-tidal delta facies. The broad channel forms, with lateral accretion surfaces and superimposed bidirectional cross-stratification that decreases

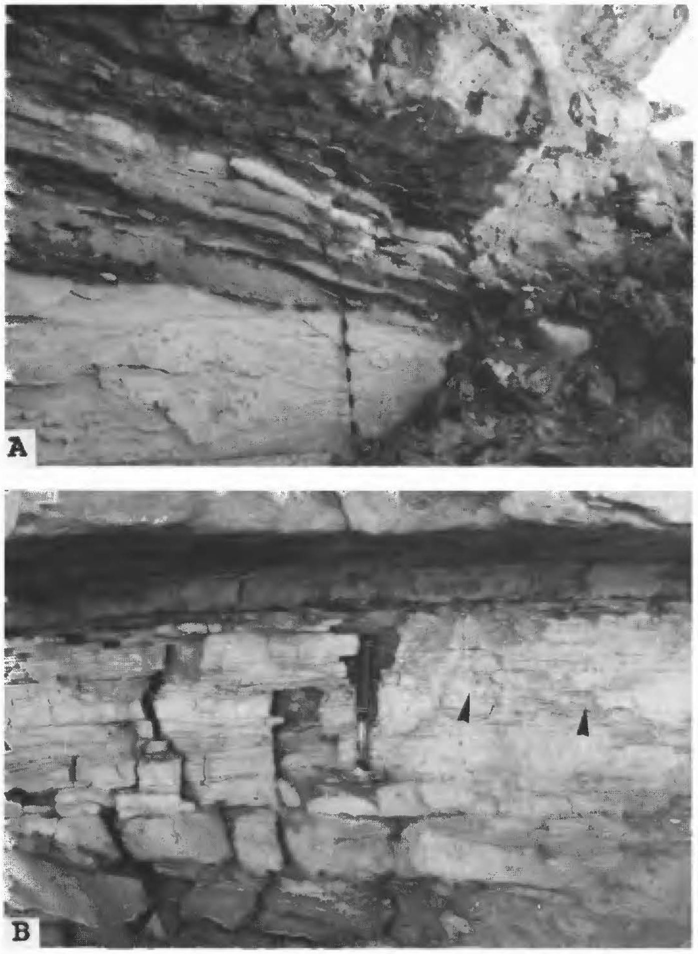

FIGURE 5. Features of LF IIb. A, Interbedded sandstone and carbonaceous siltstone and mudstone of LF IIb at a more distal position from the barrier than those shown in B. B, The thin, fine-grained sandstone beds are interpreted as washover deposits. Arrows point to the base of a scour surface.

upward in scale, are interpreted as the deposits of alongshore-migrating tidal inlets (Moslow and Heron, 1978). Alongshore and landward migration of inlets may have been responsible for removal of all or part of the lagoonal deposits. At Tanner Mesa, amalgamated inlet-fill sandstone can be traced landward into smaller channel sandstones with predominantly landward-oriented and minor seaward-oriented cross-stratification interpreted to represent ramp and channel portions of a flood tidal delta (Boothroyd and Hubbard, 1975). Distinct areas (at least 1 km wide along strike) of ebb-oriented cross-stratification in channel sandstones suggest a complex and areally extensive, tidally influenced channeled estuary (Greer, 1975; Barwis and Makurath, 1978).

Lithofacies III

Description

LF III achieves a maximum thickness of 1.5 m, and is composed predominantly of finely laminated siltstone with common, thin (<10 cm) sandstones. It occurs disconformably overlying LF Ia shoreface sandstone facies (Fig. 7). Thin sandstones within the unit are hummocky cross-stratified and parallel laminated, and are laterally discontinuous over distances of less than 10 m. Tool marks showing predominantly offshore orientations are common on the base of sandstone beds, and the bases and tops of sandstones are commonly bioturbated with the trace fossils *Planolites* and *Thalassinoides*. Rare *Chrondrites* occur in mudstones. Scour-and-fill structures in both sandstones and mudstones are typical. Where present, LF III is laterally discontinuous along depositional dip over distances of less than 1 km.

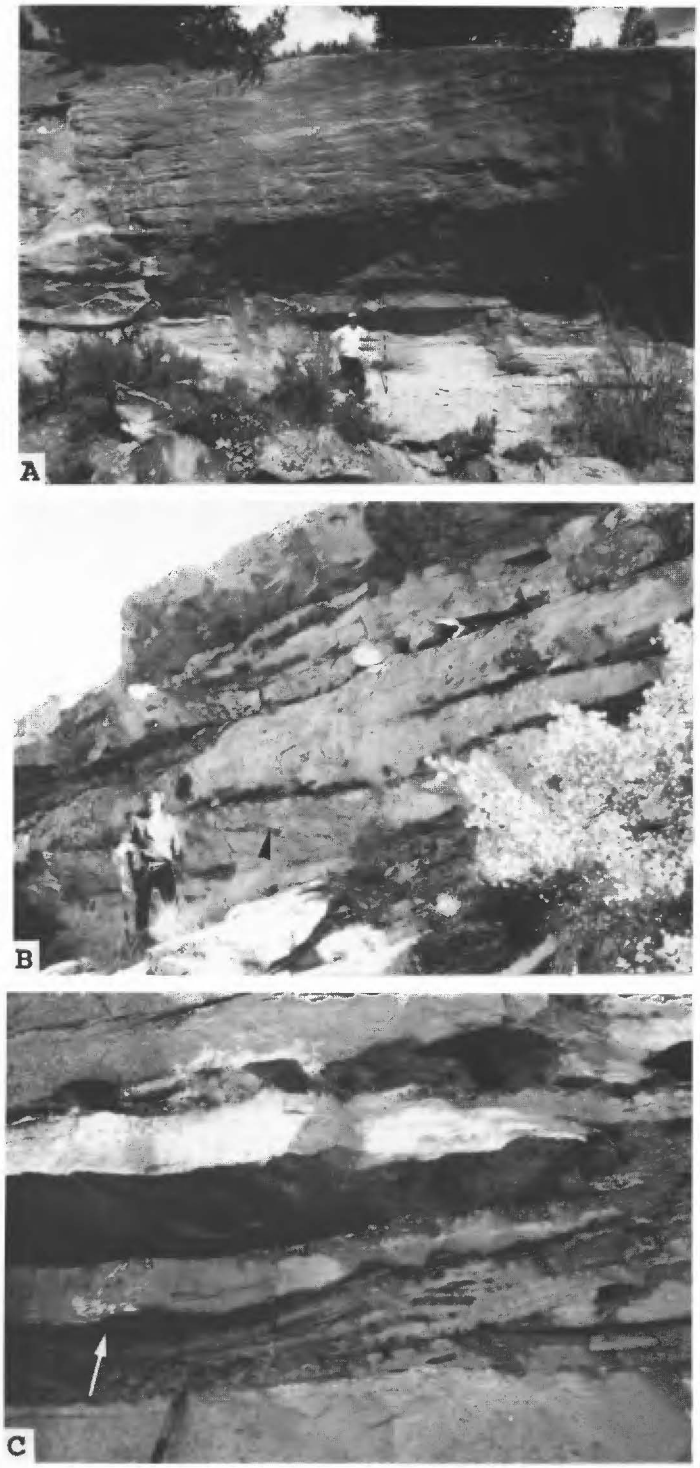

FIGURE 6. Subenvironments of LF IIc. A, Inlet-fill sandstone with abundant bidirectional crossbedding at Moqui Canyon. Large-scale inclined bedding (dipping to the left of photo) resulted from lateral migration of a tidal inlet. B, Ramp portion of a flood tidal delta at Tanner Canyon; arrow points to landward-directed crossbeds. C, Thin channel of distal flood tidal delta, interfingering with lagoonal deposits of LF IIb.

Interpretation

Rocks of LF III are interpreted to represent deposition in the shoreface to inner-shelf transition zone. Scour-and-fill features, found throughout LF III, and hummocky cross-stratified sandstones suggest that these sediments were frequently subjected to storm waves. The lack of continuous or amalgamated sandstone beds, and the presence of mudstones,

FIGURE 7. Transgressive mudstone of LF III overlying shoreface sandstone at measured section 9, Fig. 10.

many of which are scoured, suggest that LF III represents deposition in deeper water than shoreface sediments of LF Ia (but still above storm wave base), or that they may represent deposition in water depths equivalent to LF Ia, but with either restricted sand supply or decreased energy during deposition.

Lithofacies IV

Description

Lithofacies IV consists predominantly of very fine- to fine-grained sandstones and minor shale and silty shale, and disconformably overlies LF Ia shoreface sandstone (Fig. 8). Individual sandstone bodies are laterally discontinuous over distances of <100 m along depositional strike and dip. Thick (1–4 m) sandstone beds typically divide laterally along depositional strike into thinner sandstones with interbedded shales. Hummocky and swaley cross-stratification and sandstone beds that drape over each other characterize LF IV. Shale and silty shale intervals display scour-and-fill structures (Fig. 9), and commonly become increasingly more carbonaceous upward within LF IV. Trace fossils characteristic of LF IV are *Planolites* and *Thalassinoides*. Bioturbation in LF IV is most abundant at sandstone/shale contacts, but occurs throughout the lithofacies. In Mancos Canyon, LF IV thickens eastward from 0 m to 18 m before the unit (and the entire Point Lookout) dips into the subsurface.

Devine (1980, 1991) described a similar facies (Unit T), in the Point Lookout Sandstone in northwestern New Mexico, as being composed of fine-grained sandstone and siltstone. Sedimentary structures consist of trough cross-stratification interbedded with subhorizontal, subparallel laminations. Unit T is laterally continuous, 13 to 18 m thick, and pinches out in the landward direction in a manner similar to LF IV. The trend of the landward pinchout of Unit T diverges from the regional shoreline trend by up to 30°.

Qualitative petrographic analysis of LF IV indicates that sparry calcite cement and early authigenic dolomite grains are more common in sandstones of LF IV than in shoreface sandstone (LF I). In addition, sandstones of LF IV are better sorted than shoreface sandstone, because of the absence of the mud-sized fraction.

Interpretation

LF IV represents deposition of shoal-like sand bodies on the inner shelf. Sedimentary structures and sandstone bed geometries suggest that the shoal complex was deposited and reworked predominantly by storm processes (Harms, 1975). Overall seaward thickening of the inner-shelf sandstone represents the two-dimensional aspect of the unit, but the extent to which the unit rests in topographic (erosional) lows on the inner shelf or forms positive relief is uncertain. Thinning of shoreface

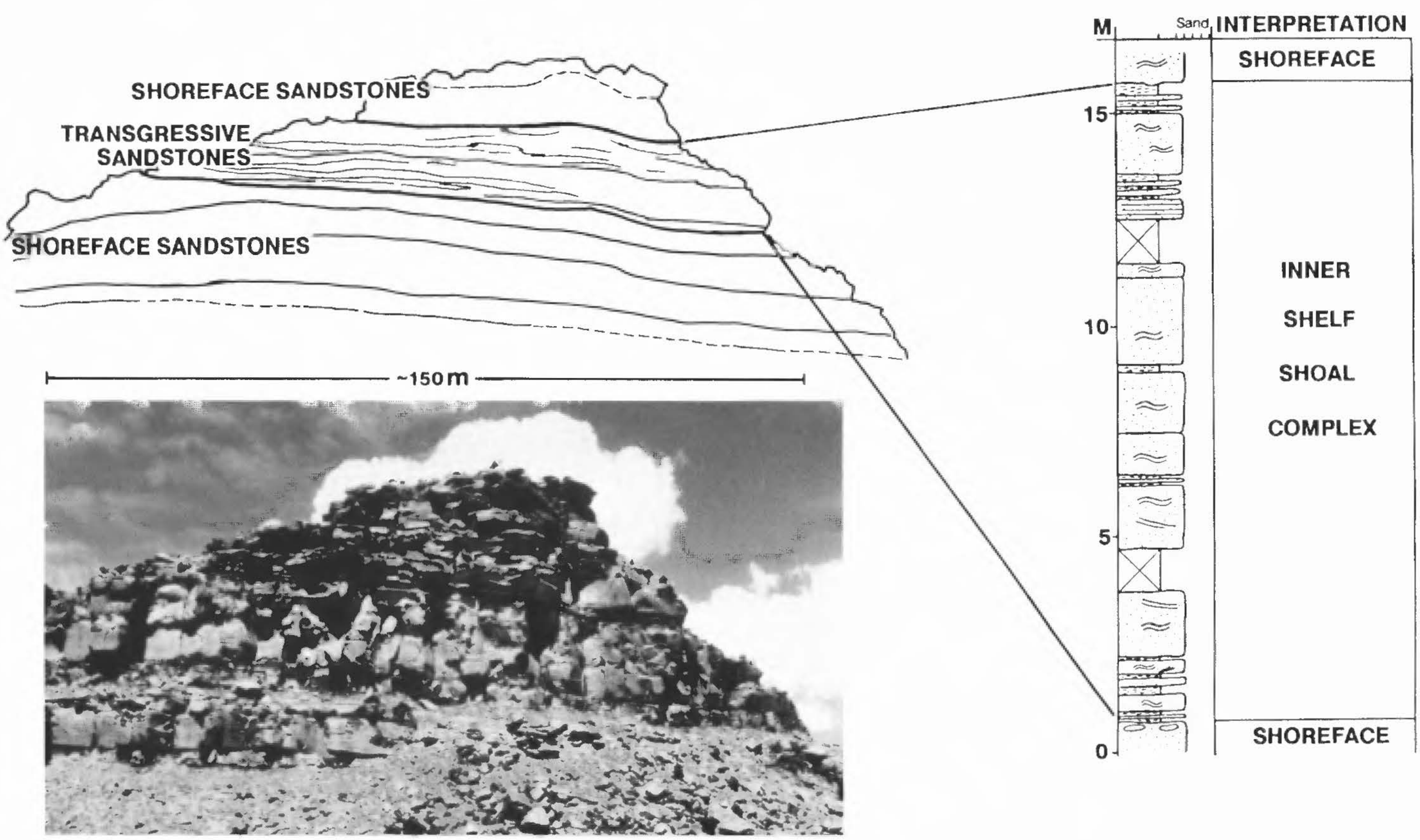

FIGURE 8. Photo and line sketch showing transgressive inner-shelf sandstones (LF IV) in sharp contact with underlying and overlying parasequences (shoreface sandstone of LF Ia). The measured section illustrates the internal nature of LF IV.

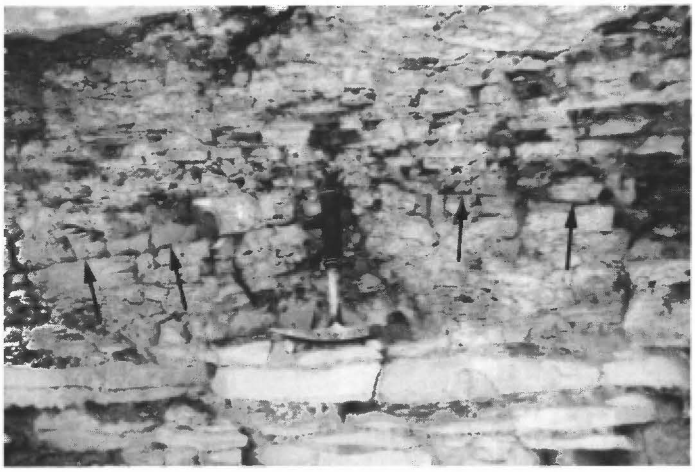

FIGURE 9. Scour-and-fill structures in shale and silty shale portion of LF IV. Arrow points to scour surfaces.

sandstones above and below suggests a combination of both. The minor mudstone found intercalated with thicker sandstones is probably related to deposition of fine-grained sediments in calmer water along the flanks of the shoals. Better sorting of the sandstones (compared to regressive sandstones) may result from winnowing of the mud fraction by repeated storm reworking. The sparry calcite cement is probably a diagenetic product related to later influence of meteoric waters; however, good sorting and consequent high permeability allowed preferential access to meteoric waters.

Sabins (1962) described offshore increasing abundance of primary dolomite in Cretaceous sandstones in the Western Interior. Primary dolomite are grains "formed within the depositional basin and were present as dolomite prior to the final settling-down and burial of the sediment" (Sabins, 1962, p. 1185). Although the nature of the formation of primary dolomite on the seafloor is not well understood, there are two possible explanations for the greater abundance observed in the inner-shelf sandstones in the Point Lookout Sandstone. One mechanism is lag-concentration during reworking of dolomite-bearing regressive sandstones by the ravinement process. Alternatively an offshore position of the shoal complex may have allowed more widespread formation of primary dolomite, which was subsequently reworked and deposited in the transgressive sandstones. In either case, the greater abundance of dolomite and the good sorting in the inner-shelf sandstones (LF IV) provides a means of distinguishing LF IV from other lithofacies (e.g., shoreface sandstone, LF Ia).

CYCLE ELEMENTS, GEOMETRY, AND MODE OF DEVELOPMENT

A cross section (Fig. 10) through the Point Lookout Sandstone in Mancos Canyon illustrates the vertical and lateral facies relationships and the stacking pattern of parasequences and parasequence sets. The line of section is southwest to northeast, roughly perpendicular to the strike of shorelines at Tanner Mesa and Moqui Canyon (Fig. 2). We now focus on the facies architecture of parasequences and parasequence sets in terms of their physical characteristics, stratigraphic relationships and mode of development.

Point Lookout progradational parasequences are grouped into progradational parasequence sets (Fig. 10). These two cycle scales are delineated primarily on the basis of lithologic characteristics and thickness of offshore transgressive deposits that occur at cycle boundaries. At the parasequence scale, offshore transgressive deposits are represented by thin LF III mudstone; at the parasequence-set scale, offshore transgressive deposits are represented by a variably thick (0 to 20 m) interval of sandstone and minor intercalated mudstone (LF IV). Retrogradational and progradational back-barrier deposits also occur as im-

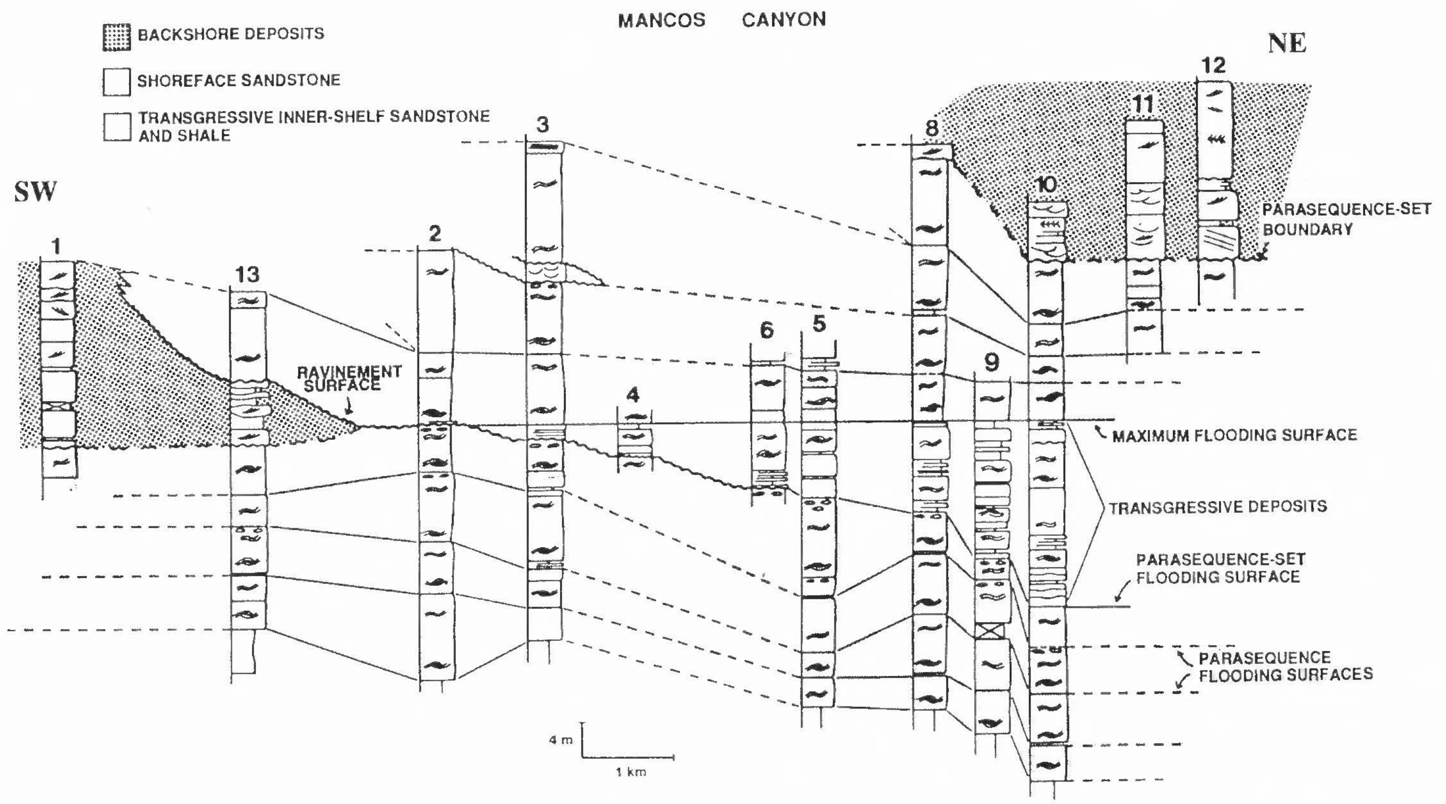

FIGURE 10. Cross section through Mancos Canyon illustrating Point Lookout Sandstone facies architecture. The datum for the section is the parasequence-set maximum flooding surface. Parasequences are shown in the lightly shaded area and are grouped into sets of four regressive shoreface sandstones (LF Ia) and corresponding transgressive surfaces and deposits (LF III). These grouped parasequences comprise the regressive portion of a parasequence set. Unshaded area represents transgressive inner-shelf deposits of LF IV. Inner-shelf deposits and four adjacent (overlying) parasequences comprise a parasequence-set transgressive-regressive cycle. Darkly shaded area corresponds to regressive and transgressive backshore deposits of LF IIa–c.

portant elements of parasequences and especially parasequence sets. As with offshore transgressive deposits, thickness of back-barrier deposits is a key characteristic for distinguishing parasequence and parasequence-set boundaries. The progradational nature of the parasequences and parasequence sets in the Point Lookout, coupled with stratigraphic rise, place these strata within the highstand systems tract position of van Wagoner et al. (1988).

Parasequences

The lightly shaded area in Fig. 10 shows the regressive portions of two parasequence sets, each set being composed of four parasequences. In outcrop, individual parasequences are expressed as coarsening-upward tabular sandstone bodies (LF Ia), that are 3 to 7 m thick, and laterally traceable for kilometers in strike and dip directions. These sheet sandstones are abruptly overlain by a marine-flooding surface with either thin (<1 m) mudstone (LF III) and/or lag deposits and calcareous concretions.

As discussed earlier, transgressive mudstones (LF III) lie disconformably above and below regressive shoreface sandstones of LF Ia. The lower and upper transition from LF III to LF Ia within each parasequence is abrupt, not gradational as would be expected for the distal portion of a prograding shoreface. This is also the case where concretions mark the boundary between parasequences. Here, it is important to emphasize that mud deposition (LF III) on the underlying shoreface during transgression (i.e., landward translation of the mudline) did not necessarily correspond with equal landward translation of the shoreline. In only one location in the study area are fluvial or tidal channels of LF IIa found beneath foreshore or shoreface deposits (Fig. 10, section 3) suggesting that, at this scale, there was little landward shift in shoreline position during transgression. It is, therefore, doubtful that the change from shoreface sandstone of LF Ia to interbedded sandstone and mudstone of LF III represents significant change in water depth. Rather, the abrupt change from LF Ia to LF III suggests a decrease in sand supply to the innermost shelf and possibly, decreased intensity or frequency of storm events so that not all fairweather mud was eroded during these events. Periods of increased sand supply caused renewed progradation of the shoreface, resulting in the sharp-based nature of the overlying regressive sandstone (LF Ia) (Fig. 10).

LF III, therefore, is interpreted to represent deposition of interbedded sandstone and mudstone on the underlying shoreface during very minor transgressive events. Reduction in marine sand supply may have resulted from small-scale back-barrier flooding without a significant landward shift in barrier position. Coarse sediment was temporarily trapped behind the beach, while mud could have been transported either through the small estuaries or along shore.

Coastal-plain deposits preserved at parasequence boundaries are generally thin (<2 m) fluvial or tidal channels (LF IIa), which may have formed either during progradation or as late-stage estuarine fill following transgressive flooding. No evidence of fine-grained back-barrier lagoon or bay deposits has been observed at this scale, but preservation of these units on eroded cliff tops is unlikely. Also, such deposits would have little preservation potential if migratory tidal channels succeeded estuarine deposition. Lateral migration of fluvial and tidal creeks like these is also responsible for removal of foreshore deposits in modern settings (Barwis and Hayes, 1979) and probably explains the rarity of preserved parasequence-scale foreshore deposits in the study area.

Parasequence sets

Within the study area, two distinct basinward-stepping (progradational) packages of cliff-forming sandstone (Fig. 10), each composed of four parasequences, represent the regressive portion of parasequence sets (Fig. 10). The "bundling" of four parasequences within a parasequence set was observed in two parasequence sets within the study area. A similar hierarchy was also observed by Devine (1980, 1991) in northwestern New Mexico, although scale nomenclature varies between those studies and this one. These cliff-forming sandstones are sharp based over distances of approximately 10 km in the offshore direction, where the transition to offshore mudstone, in the stratigraphically lowest parasequence, occurs over a narrow zone less than 1 km wide.

The regressive portion of a parasequence set is abruptly overlain by the parasequence-set marine-flooding surface which merges with the ravinement surface in the landward direction. Disconformably overlying the marine-flooding surface is inner-shelf sandstone and mudstone of LF IV (unshaded portion in Fig. 10). A thin (<0.5 m) highly bioturbated basal-lag deposit occurs locally.

LF IV is the facies that delineates the parasequence-set boundary in the offshore position. LF IV thickens from 0 m at section 2 to 20 m at section 10 (Fig. 10) where the unit dips into the subsurface. Inner-shelf sandstone and mudstone of LF IV are genetically unrelated to overlying or underlying shoreface sandstones (LF Ia) because LF Ia and LF IV do not interfinger. This stratigraphic relationship, together with the textural differences between LF Ia and LF IV (see lithofacies section), suggests that LF IV represents deposition on the inner shelf during transgression.

The occurrence of inner-shelf transgressive deposits (LF IV) requires consideration of the source of sand that is compatible with the volume of sand and grain-size range found in Point Lookout inner-shelf sandstones. Explanations for morphologically similar Holocene transgressive inner-shelf sands include: (1) erosion and redistribution of shoreface deposits during shoreface retreat (Swift, 1968; Nummedal and Swift, 1987); (2) reworked estuary-mouth sediments (Swift et al., 1978; Swift et al., 1984); and (3) drowned barrier islands (Rampino and Sanders, 1980). The last model is discounted because Point Lookout inner-shelf sandstones rest unconformably on older shoreface sandstones, rather than being in contact with back-barrier facies.

The two-dimensional geometry of the inner-shelf sandstone exposed in Mancos Canyon is similar to that described for "shoal retreat massifs" (Swift, 1975; Swift et al., 1978) along the Atlantic coast, where estuary-mouth sands were reworked into a ridge-and-swale topography on the inner shelf during transgression. Point Lookout shelf sandstones (LF IV) did form seaward of contemporaneous estuaries (LF II), but only the dip-aligned orientation of the transgressive inner-shelf sandstone in Mancos Canyon is well constrained, precluding direct comparison to Swift's examples. In a subsurface study of the Point Lookout in northwestern New Mexico, however, Devine (1980, 1991) described transgressive inner-shelf sandstones that lie on what we interpret as the parasequence-set boundary directly beneath the one studied in Mancos Canyon. Excellent well-log control allowed Devine to constrain the strike-aligned geometry of the transgressive sandstone, which compares well with Swift's examples. The problem with applying Swift's (1975) model to the Point Lookout is that grain sizes in the inner-shelf sandstone in Mancos Canyon are not compatible with the 250–350 micron sand characteristic of estuary deposits in the Point Lookout.

Another possible source of sand for the inner-shelf sandstones is sediment transport alongshore from a position along strike that was not undergoing transgression (and associated reduction in sediment supply). A large prograding delta near the retrograding shoreline in the study area may have provided sediment for longshore transport along the inner shelf. The orientations of tool marks throughout the study area suggest, however, a more offshore than alongshore transport direction.

We favor an explanation for the Point Lookout inner-shelf sandstone (LF IV) involving sand derived from ravinement of older shoreface deposits during shoreface retreat, with both landward and seaward redistribution of sediment (Niedoroda et al., 1985; Kraft et al., 1987). This process would redistribute lower shoreface sediments seaward, producing sand bodies with grain sizes compatible with those in the Point Lookout inner-shelf shoal complex. The coarser-grained sands of the eroded upper shoreface and beach were, however, consequently retained in nearshore environments where tidal deposits (LF II) have grain sizes and textures compatible with recycled upper shoreface and foreshore deposits. Leatherman (1985) suggested that tidal inlets on Fire Island, New York, played a similar role in the net landward transfer of eroded barrier sands during the Holocene transgression.

Back-barrier deposits (LF II) at the parasequence-set scale are represented by extensive tidal deposits preserved at the maximum retrograde shoreline position. Thick accumulations (up to 15 m) of various tidal subenvironments are the expression of transgressive (aggradational) facies at parasequence-set boundaries. At section 13 (Fig. 10), channel deposits (LF IIa) approximately 4 m thick are preserved beneath shoreface sandstone (LF Ia), approximately 2 km seaward of the position of the shoreface at maximum transgression. A ravinement surface separates the two facies. A complete vertical sequence of back-barrier deposits (Fig. 11) consists of basal fluvial and tidal channels (LF IIa), overlain by lagoonal deposits (LF IIb), overlain by tidal-inlet and tidal-delta deposits (LF IIc) (Fig. 4B). In all cases, these tidal deposits grade upward into foreshore or swash platform facies (LF Ib) that pass seaward into shoreface sandstone (LF Ia) of the lowermost parasequence of a younger parasequence set.

Fig. 12 schematically illustrates coastal-plain evolution inferred to produce the back-barrier sequence mentioned above. This sequence represents the onset of transgression as (initially progradational) fluvial and tidal creeks (basal LF IIa) aggraded in response to the first signs of baselevel rise. Eventually, the coastal plain was inundated, and the site of fluvial deposition shifted landward as a lagoon formed immediately landward of the retrograding barrier. As the barrier continued to move landward, various tidal facies of LF IIc developed and interfingered with or truncated the lagoonal deposits. This sequence represents aggradation and retrogradation of various nearshore environments in response to relative sea-level rise. These transgressive back-barrier deposits (LF IIa–c) are interpreted to be time-equivalent with the transgressive inner-shelf sandstones of LF IV.

Detailed resolution of the geometry of each individual cycle element in the Point Lookout allows the construction of chronostratigraphic and lithostratigraphic models that illustrate the facies distribution in time and space, respectively (Fig. 13). The models illustrate the shoreface stacking patterns of progradational parasequences into progradational parasequence sets and the location of transgressive deposits at cycle boundaries. The presence of transgressive deposits is a key aspect of the models. This is in contrast to "classic" parasequence models that state that transgressive deposits are not important in parasequence stratigraphy.

CONCLUSIONS

High-frequency depositional cycles in the Point Lookout Sandstone in southwestern Colorado and northwestern New Mexico record the stacking of four progradational parasequences into each of three progradational parasequence sets. This stacking pattern places the Point Lookout Sandstone in the study area within the highstand systems tract position.

Transgressive deposits are an important component of parasequences and parasequence sets. At parasequence boundaries, transgressive deposits consist of thin (<1 m) mudstone-dominated intervals and/or lag deposits. At parasequence-set boundaries, thick (up to 20 m) transgressive deposits lie at both back-barrier and inner-shelf positions. In the back-barrier, a 15-m-thick section represents environments progressing upward from fluvial- and tidal-creek sandstones into small lagoon or pond deposits erosionally overlain by tidal inlet, tidal delta and tidal channel (estuarine) deposits. This sequence is retrogradational, and is therefore assigned to the transgressive portion of the cycle.

On the inner shelf, shoal-like sandstone bodies and minor intercalated mudstone form a seaward-thickening (0–20 m) shoal complex. These deposits are considered genetically unrelated to underlying and overlying shoreface sandstones, and are therefore interpreted as transgres-

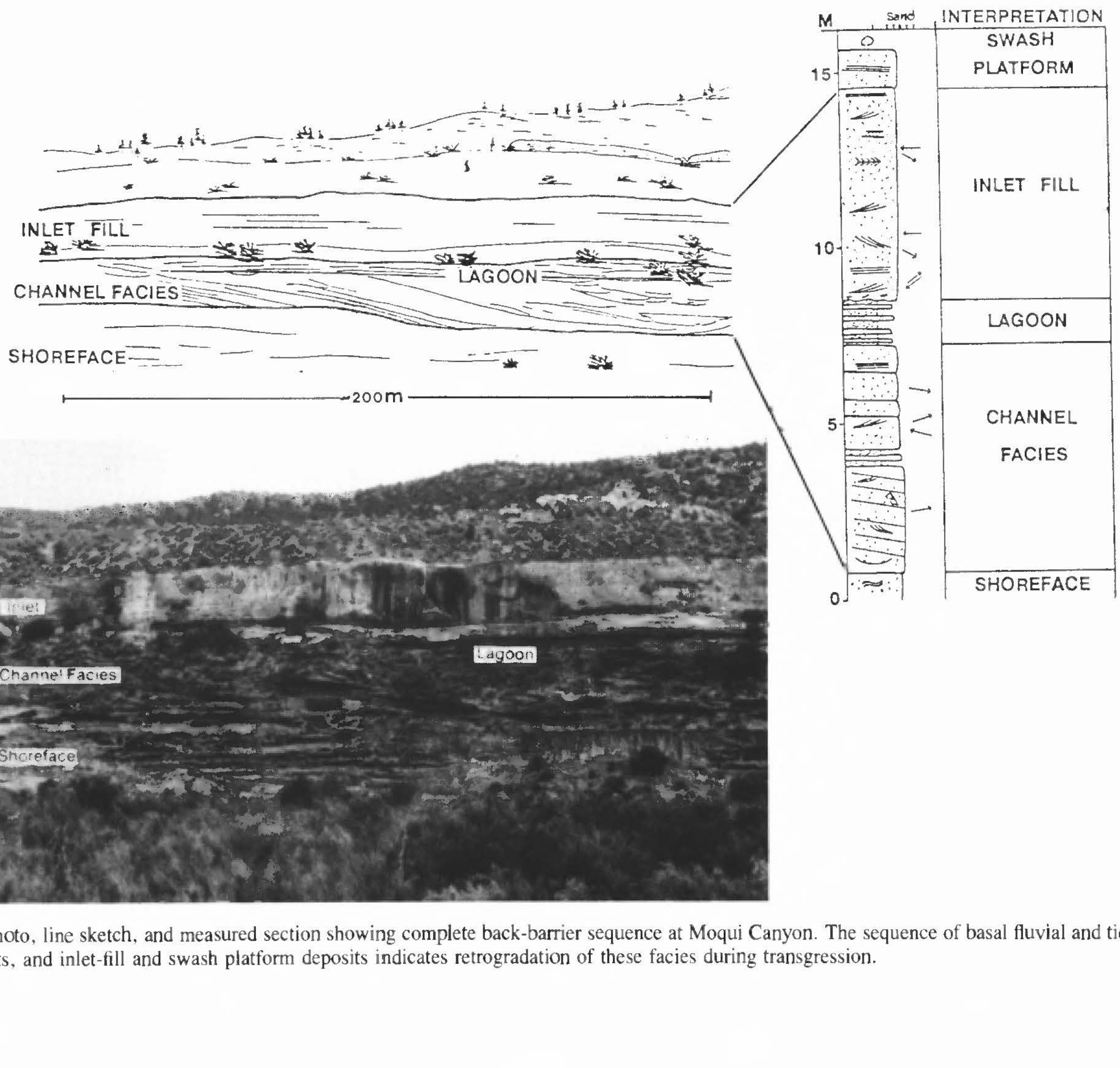

FIGURE 11. Photo, line sketch, and measured section showing complete back-barrier sequence at Moqui Canyon. The sequence of basal fluvial and tidal channels, lagoonal deposits, and inlet-fill and swash platform deposits indicates retrogradation of these facies during transgression.

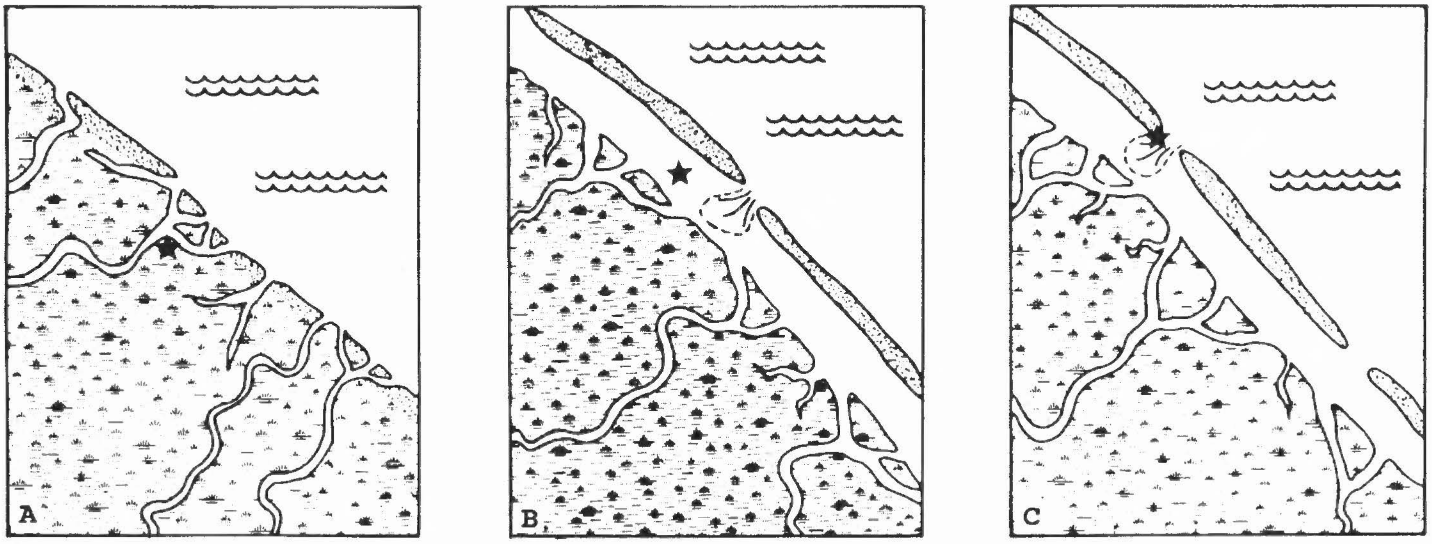

FIGURE 12. Schematic model of shoreline and backshore evolution that produces the back-barrier sequence shown in Fig. 11. Star corresponds to location of measured section 1 (Fig. 2). At the location of the star, the depositional environment progresses from (a) fluvial and tidal channels to (b) lagoon to (c) tidal inlet and flood tidal delta deposition.

sive. Their position on the inner shelf, directly offshore of transgressive back-barrier (estuarine) deposits, suggests coeval deposition of the two facies. The source of sand for the inner-shelf sandstone is problematic. A model that incorporates ravinement of shoreface sand during transgression with distribution of the sand both landward (to be incorporated into tidal deposits) and seaward onto the inner shelf is suggested to explain the formation of the inner-shelf shoal complex in the Point Lookout Sandstone.

Individual sandstone beds within the inner-shelf shoal complex are laterally discontinuous over distances of 100 m, unlike shoreface sandstones (regressive portion of a parasequence) that are laterally continuous for kilometers in strike and dip directions. The overall lens-like geometry of the inner-shelf shoal complex is distinguished from the tabular geometry of the regressive portion of parasequences and parasequence sets. In addition, qualitative analysis of sandstone sorting and mineralogy indicate that transgressive inner-shelf sandstones can readily be distinguished from regressive shoreface sandstones based on textural characteristics.

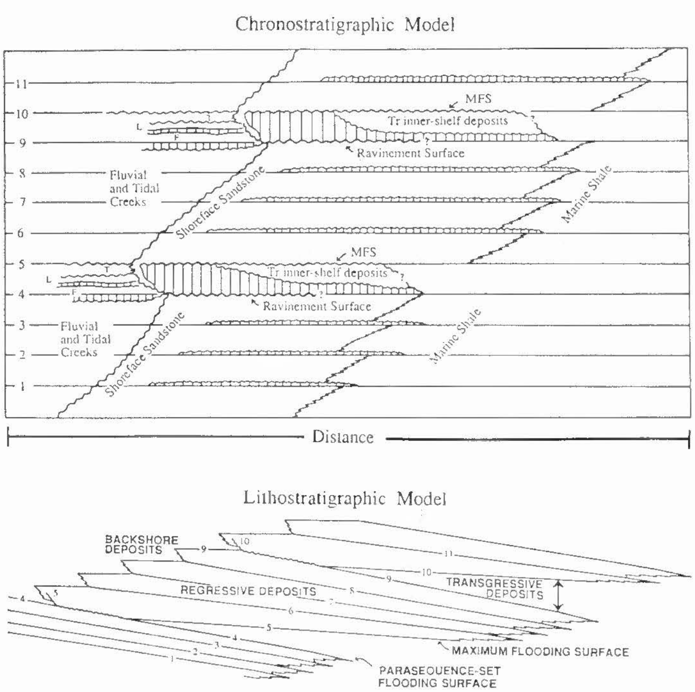

FIGURE 13. Chronostratigraphic and lithostratigraphic models for the Point Lookout Sandstone, illustrating the distribution of cycle elements and stacking patterns of progradational parasequences and progradational parasequence sets. Vertical axis on the chronostratigraphic model represents time. Time lines on both models correspond to marine flooding surfaces or maximum flooding surfaces. Equal spacing of time lines is not intended to suggest cycle periodicity. F, L and T = fluvial, lagoonal and tidal, respectively; Tr = transgressive.

ACKNOWLEDGMENTS

We express our appreciation for the valuable field and technical contributions of Gary Smith, Rob Zech, Dave Hicks and Jeff Black. Financial and logistical support was provided by British Petroleum Exploration, Inc., the Donors of the Petroleum Research Fund of the American Chemical Society, American Association of Petroleum Geologists Grants-in-Aid, New Mexico Bureau of Mines and Mineral Resources, New Mexico Geological Society, University of New Mexico Student Research Allocations Committee, the United States Geological Survey, and Sigma Xi. Special thanks to the Ute Mountain Ute Tribe and to Doug Bowman and Arthur Cuthair for permitting access to Tribal Park land.

REFERENCES

Barwis, J. H. and Hayes, M. O., 1979, Regional patterns of modern barrier island and tidal-inlet deposits as applied to paleoenvironmental studies; *in* Ferm, J. C. and Horne, J. C., eds., Carboniferous depositional environments in the Appalachian region: Columbia, South Carolina, University of South Carolina, Carolina Coal Group, 760 p.

Barwis, J. H. and Markurath, J. H., 1978, Recognition of ancient tidal-inlet sequences: an example from the Upper Silurian Keyser Limestone in Virginia: Sedimentology, v. 25, p. 61–82.

Boothroyd, J. C. and Hubbard, D. K., 1975, Genesis of bedforms in mesotidal estuaries; *in* Cronin, L. E., ed.: Estuarine Research, Geology and Engineering, v. 2, p. 167–182.

de Boer, P. L. and Wonders, A. A. H., 1984, Astronomically-induced rhythmic bedding in Cretaceous pelagic sediments near Moria (Italy); *in* Berger, A. L., et al., eds., Milankovich and Climate, Part 1, p. 177–190.

Devine, P. E., 1980, Depositional patterns in the Point Lookout Sandstone, northwestern San Juan Basin, New Mexico [M.A. thesis]: Austin, University of Texas, 238 p.

Devine, P. E., 1991, Transgressive origin of channeled estuarine deposits in the Point Lookout Sandstone, northwestern New Mexico: a model for Upper Cretaceous, cyclic regressive parasequences of the U.S. Western Interior: American Association of Petroleum Geologists Bulletin, v. 75, p. 1039–1063.

Fouch, T. D., Lawton, T. F., Nichols, D. J., Cashion, W. B. and Cobban,

W. A., 1983, Patterns and timing of synorogenic sedimentation in Upper Cretaceous rocks of central northeastern Utah; *in* Reynolds, M. W. and Dolly, E. D., eds., Mesozoic paleogeography of the west-central United States: Society of Economic Paleontologists and Mineralogists, 2nd Rocky Mountain Paleogeography Symposium, Denver, Colorado, p. 306–336.

Greer, S. A., 1975, Sandbody geometry and sedimentary facies at the estuary-marine transition zone, Ossabaw Sound, Georgia: a stratigraphic model: Senckenbergiana Maritima, v. 7, p. 105–135.

Harms, J. C., 1975, Stratification produced by migrating bedforms: *in* Depositional environments as interpreted from primary sedimentary structures and stratification sequences: Society of Economic Paleontologists and Mineralogists, Short Course 2, p. 45–61.

Harms, J. C., Southard, J. B. and Walker, R. G., 1982, Structure and sequence in clastic rocks, lecture notes: Society of Economic Paleontologists and Mineralogists, Short Course 9.

Hollenshead, C. T. and Pritchard, R. L., 1961, Geometry of producing Mesa Verde Sandstones, San Juan Basin; *in* Peterson, J. A. and Osmond, J. C., eds., Geometry of sandstone bodies: Tulsa, Oklahoma, American Association of Petroleum Geologists, p. 98–118.

Kraft, J. C., Chrzastowski, M. J., Belknap, D. F., Toscano, M. A. and Fletcher, C. H. III, 1987, The transgressive barrier-lagoon coast of Delaware: morphostratigraphy, sedimentary sequences and responses to relative rise in sea level; *in* Nummedal, D. and Pilkey, O. H., eds., Sea-level fluctuation and coastal evolution: Society of Economic Paleontologists and Mineralogists, Special Publication 41, p. 129–143.

Leatherman, S. P., 1985, Geomorphic and stratigraphic analysis of Fire Island, New York: Marine Geology, v. 63, p. 173–196.

Leckie, D. A. and Walker, R. G., 1982, Storm- and tide-dominated shorelines in Cretaceous Moosebar-Lower Gates interval—outcrop equivalents of deep basin gas trap in western Canada: American Association of Petroleum Geologists Bulletin, v. 66, p. 138–157.

Montz, M. J., Nummedal, D. and Swift, D. J. P., 1985, Shelf storm-deposited sandstones, Upper Mancos Shale, San Juan Basin, New Mexico: American Association of Petroleum Geologists Bulletin, v. 69, p. 289.

Moslow, T. F. and Heron, S. D., 1978, Relict inlets: preservation and occurrence in the Holocene stratigraphy of southern Core Banks, North Carolina: Journal of Sedimentology Petrology, v. 48, p. 1275–1286.

Niedoroda, A. W., Swift, D. J. P., Figueriredo, A. G. and Freeland, G. L., 1985, Barrier island evolution, Middle Atlantic Coast, USA, part II: evidence from the shelf floor: Marine Geology, v. 63, p. 363–396.

Nummedal, D. and Swift, D. J. P., 1987, Transgressive stratigraphy of sequence-bounding unconformities—some principles derived from Holocene and Cretaceous examples; *in* Nummedal, D. and Pilkey, O. H., eds., Sea-level fluctuation and coastal evolution: Society of Economic Paleontologists and Mineralogists, Special Publication 41, p. 242–260.

Oomkens, E., 1974, Lithofacies relations in the late Quaternary Niger Delta complex: Sedimentology, v. 21, p. 195–222.

Rampino, M. R. and Sanders, J. E., 1980, Holocene transgression in south central Long Island: Journal of Sedimentary Petrology, v. 50, p. 1063–1079.

Reinson, G. E., 1984, Barrier island and associated strandplain facies; *in* Walker, R. G., ed., Facies models: p. 119–140.

Ryer, T. A., 1977, Patterns of Cretaceous shallow-marine sedimentation, Coalville and Rockport areas, Utah: Geological Society of American Bulletin, v. 88, p. 177–188.

Sabins, F. F., 1962, Grains of detrital, secondary, and primary dolomite from Cretaceous strata of the Western Interior: Geological Society of America Bulletin, v. 73, p. 1183–1196.

Sears, J. D., Hunt, C. B. and Hendricks, T. A., 1941, Transgressive and regressive Cretaceous deposits in southern San Juan Basin, New Mexico: U.S. Geological Survey, Professional Paper 193, p. 101–121.

Swift, D. J. P., 1968, Coastal erosion and transgressive stratigraphy: Journal of Geology, v. 76, p. 444–456.

Swift, D. J. P., 1975, Tidal sand ridges and shoal retreat massifs: Marine Geology, v. 18, p. 105–134.

Swift, D. J. P., Sears, P. C., Bohlke, B. and Hunt, R., 1978, Evolution of a shoal retreat massif, North Carolina shelf: inferences from area geology: Marine Geology, v. 27, p.19–42.

Swift, D. J. P., McKinney, T. F. and Stahl, L., 1984, Recognition of transgressive and post-transgressive sand ridges on the New Jersey continental shelf: discussion; *in* Tillman, R. W. and Seimers, C. T., eds., Siliciclastic shelf sediments: Society of Economic Paleontologists and Mineralogists Special Publication 34, p. 25–36.

van Wagoner, J. C., 1985, Reservoir facies distribution as controlled by sea-level change: Society of Economic Paleontologists and Mineralogists, Midyear Meeting, Golden, Colorado, Abstracts, p. 91–92.

van Wagoner, J. C., Posamentier, H. W., Mitchum, R. M. Jr., Vail, P. R., Sarg, J. F., Loutit, T. S. and Hardenbol, J., 1988, An overview of the fundamentals of sequence stratigraphy and key definitions; *in* Wilgus, C. K. et al., eds., Sea-level changes: an integrated approach: Society of Economic Paleontologists and Mineralogists, Special Publication 42, p. 39–45.

van Wagoner, J. C., Mitchum, R. M., Campion, K. M. and Rahmanian, V. D., 1990, Siliciclastic sequence stratigraphy in well logs, cores, and outcrops: concepts for high-resolution correlation of time and facies: American Association of Petroleum Geologists, Methods in Exploration Series, no. 7.

Wright, R., 1984, Paleoenvironmental interpretation of the Upper Cretaceous Point Lookout Sandstone: implications for shoreline progradation and basin tectonic history, San Juan Basin: New Mexico [Ph.D. dissertation]: Houston, Texas, Rice University, 404 p.

Wright, R., 1986, Cycle stratigraphy as a paleogeographic tool: Point Lookout Sandstone, southeastern San Juan Basin, New Mexico: Geological Society of America Bulletin, v. 96, p. 661–673.

Wright, R., 1988, Cycle stratigraphy; *in* Nummedal, D., Wright, R. and Swift, D. J. P., eds., Sequence stratigraphy of Upper Cretaceous strata of the San Juan Basin, New Mexico: 73rd Annual Meeting, American Association of Petroleum Geologists/Society of Economic Paleontologists and Mineralogists, Field Guide, Houston, Texas, p. 134–143.

Wright, R. and Hayden, S., 1988, Point Lookout cliffs: high-order sequences (parasequences) along San Luis Road; *in* Nummedal, D., Wright, R. and Swift, D. J. P., eds., Sequence stratigraphy of Upper Cretaceous Strata of the San Juan Basin, New Mexico: 73rd Annual Meeting, American Association of Petroleum Geologists/Society of Economic Paleontologists and Mineralogists, Field Guide, Houston, Texas, p. 109–112.

Aerial view from an elevation of approximately 10,500 feet of The Hogback south of NM Highway 550. The hogback exposes Upper Cretaceous Mesaverde Group and marks the western edge of the San Juan Basin. The sinuous line near the bottom of the photograph is the San Juan River, and U.S. Highway 550 is visible just below the river. Photograph taken the morning of 13 April 1992.